Scientific Research Publishing

Journal of Modern Physics, 2025, 16(6), 843-857
https://www.scirp.org/journal/jmp
ISSN Online: 2153-120X
ISSN Print: 2153-1196

Quark Masses, Black Neutron Stars and SSI Conception of the Universe

F. C. Hoh

Retired, Dragarbrunnsg. 55, Uppsala, Sweden
Email: hoh@telia.com

How to cite this paper: Hoh, F.C. (2025) Quark Masses, Black Neutron Stars and SSI Conception of the Universe. *Journal of Modern Physics*, **16**, 843-857.
https://doi.org/10.4236/jmp.2025.166044

Received: April 12, 2025
Accepted: June 17, 2025
Published: June 20, 2025

Abstract

Recently, it was found that a quark's mass in the scalar strong interaction hadron theory SSI can deviate from some mean value within certain limits, depending upon the flavor and spin of its companion antiquark in a meson. Here, such values and limits are determined and specified with greater accuracy that led to improved predictions of meson masses. The black neutron star recent observed in the kilonova S250206dm confirms the 2019 SSI prediction of such an object. This prediction has been further developed to a "peach" model for conventional black holes. A neutron star at the verge of its Tolman, Oppenheimer, Volkoff limit replaces the gravitational singularity in the expected black hole. Such a black object, including supermassive such, is actually a black neutron star with a dense core of a neutron star of about 3.65 solar masses and a 10.8 km radius. Our present conception of the basic forces and their relations in the universe based upon the standard model is hereby modified to accommodate SSI.

Keywords

Scalar Strong Interaction Hadron Theory SSI, Ground State Mesons, Meson Mass Formula, Variable Quark Masses, Predicted Meson Masses, S250206dm Kilonova, Tolman-Oppenheimer-Volkoff (TOV) Limit, Black Neutron Star, Replacement of Gravitational Singularity, "Peach Model", Basic Forces in SSI Universe, Standard Model

1. Introduction

The basic ground state meson spectra [1] cannot be accounted for by the current mainstream standard model SM ([2] standard model). The scalar strong interaction hadron theory SSI ([3] Ch 5) is far more successful in this respect. Recent work has shown that a quark's mass obtained from meson spectra is not a natural

constant, like the electron or muon mass, but can deviate from some mean value within certain limits, dependent upon the flavor and spin of its companion antiquark [4]. Such mean values have however not been specified and the limits given are too coarse. These two shortcomings are addressed to in Section 2.

In the recent kilonova observation S250206dm, the expected black hole was not found. Instead, a black neutron star was seen, in accordance with an SSI prediction ([3] Ch 15), ([5] Sec. 7). This prediction is extended to hold for heavier black neutron stars, including supermassive such, and to provide a new conception of the conventional black holes. This is carried out in Section 3.

In Section 4, our present conception of the fundamental forces and their relations in the universe based upon SM is modified to accommodate SSI.

2. Variable Quark Masses

2.1. Background

The basic meson spectra [1] have largely been accounted for using the formula

$$E_{Jn} = \pm\sqrt{\left(m_p + m_r\right)^2 - 4d_{m0} + 8d_h\left(s + n' + \frac{3}{2}\right)},\ \ s = J \tag{1}$$

in SSI ([3] (5.1.1)). Here E_{Jn} is the strong interaction meson mass, m_p the quark masses with $p = 1, 2, 3, 4$, and 5 referring to the u, d, s, c, and b quarks, respectively. d_h is the confinement strength and d_{m0}, a "zero-point strong potential", between the quark and antiquark. $J = 0$ for pseudoscalar 0^- and $J = 1$ for vector 1^- mesons. n' is a radial quantum number. This formula is derived from meson wave equations in the "hidden", relative space between the quarks interacting via strong interaction. Mass contribution from the charges of the mesons does not enter this formula,

The 5 quark masses and the 2 constants d_h and d_{m0} have been obtained from (1) using 7 meson masses. Practically, d_h has been fixed by an average of the differences between the squares of the masses of 0^- meson and their 1^- meson partner and turns out to be 0.07 GeV^2 ([3] (5.2.2)). Thus, 6 mesons are needed to fix the 5 quark masses and d_{m0}.

From the 5 quarks and their antiquarks, we can form 25 0^- mesons and 25 1^- mesons. The isosinglet 0^- mesons $\bar{u}u$, $\bar{d}d$, $\bar{s}s$, $\bar{c}c$, and $\bar{b}b$ are forbidden (see the U(1) problem ([3] pp. 66-69)). The isosinglet 1^- meson $\omega(782)$ may contain $\bar{u}u$, $\bar{d}d$ and the sum of them divided by $\sqrt{2}$ but the proportions among them are uncertain. It is therefore excluded. Some of the remaining 44 mesons further drop out for various reasons. Putting together the + and – charged mesons into one with charge ± and using 6 neutral mesons to fix the 5 quark masses and d_{m0}, there were 16 meson masses available for test of (2) in the following section.

2.2. Previous Results [4]

There are however a huge number of ways to choose these 6 mesons; different choices yield different quark masses. Inasmuch as meson masses are known to an

accuracy of 6 digits, one may hope to obtain the quark masses with the same accuracy. In a recent paper [4] aimed at such an accuracy, however, it was found that the Coulomb contributions from the charged mesons will greatly affect such accuracy. Such contributions depend upon the charge radius of these mesons. But such radii have been measured only for pion and kaon.

To avoid such uncertainties, only neutral mesons were chosen. Since the 1^- mesons have much larger width, the 0^- mesons were chosen firsthand. But there are only 5 neutral 0^- mesons; the η's were excluded because they contain more than 2 quarks. The 6th has to come from 1^- mesons. Most of them have large widths. The best ones are the 3 isoscalars $\phi(1020)$, J/ψ and $Y(1S)$. These have been chosen in 3 different cases. In another case, 2 such 1^- mesons were chosen. Including earlier quark masses used, there were 7 different meson combinations to fix 7 sets of quark masses and d_{m0}.

The so-obtained quark masses were used to predict the masses of the above 16 remaining mesons, which include charged ones. For this purpose, (1) with $n' = 0$ had been extended to include contributions from the charges according to

$$\left(E - E_{10}\right)^2 = \left(m_p + m_r\right)^2 - 4d_{m0} + 8d_h\left(J + \frac{3}{2}\right) \tag{2a}$$

$E = E_{Jn}$ in (1) with $n' = 0$ for ground state 0^- and 1^- mesons

$$E_{10} = Q^2/R_m, \quad R_m = r_m\sqrt{\pi/2}$$

$\pi^{\pm}$: $r_m = 0.659$ fm, $E_{10} = 2.467$ MeV.

$K^{\pm}$: $r_m = 0.56$ fm, $E_{10} = 2.904$ MeV.

All other charged mesons: r_m are unknown.

$E_{10} = 2.904$ MeV is assumed for all other charged 0^- mesons.

$E_{10} = 0$ is assumed for all charged 1^- mesons because they are much heavier.

Q is the meson charge. R_m is the radius of a "marble" model of the meson charge ([5] Sec. 5). (2b)

The results show that the quark mass and d_{m0} values are not natural constants with fixed values like the masses of leptons. Such values for each Case can deviate from some "mean value" by up to ~±10% and still yield approximate meson masses. If the deviations become much larger, then the predicted masses will deviate more from their "mean values".

In SSI, therefore, quark mass and d_{m0} values are indefinite and variable and can assume values within some limits. They lead to good predictions for mesons having similar quark content as the input mesons that give rise to their values. For other mesons, the predictions are more approximate.

However, the above "mean values" have not been specified. Also, the above ±10% deviation from such "mean values" also does not tell which Case it refers to.

The purpose of this section is to tighten up the above treatments [4] and provide specific values of the "mean values" of the quark masses that agree best with data as well as the smallest deviations of the predicted quarks masses from such "mean values". Accurate quark masses are important because they see used in the baryon

sector of SSI and affect the predictions there.

2.3. Neutral Input Mesons and Quark Masses

The 7 Cases A, B, … G in Table 1 of [4] have been updated and extended to 9 Cases in Table 1.

Table 1. Input mesons for quark masses and d_{m0} from (2) for Cases B to I. The bold faced lines of Cases D and E are used as "mean masses" of the quarks to predict 18 meson masses in Tables 2-4 to confront data [1].

Case	Input mesons
A	Particle Data Group [1]
B	0^- mesons $\pi^{\pm}$, $K^{\pm}$, K^0, D^0, $D_s^{\pm}$, and B^0 with E_{10} = 2.1 MeV in approximative ([3] Table 5.2)
C	Same mesons as in B but using (2) and obtained systematically with 6 digit accuracy
D	Neutral mesons π^0, K^0, D^0, B^0, B_s^0, and $\phi(1020)$
E	Neutral mesons π^0, K^0, D^0, B^0, B_s^0, and J/ψ
F	Neutral mesons, π^0, K^0, D^0, B^0, B_s^0, and $Y(1S)$
G	Neutral mesons K^0, p^0, D^0, B^0, B_s^0, $\phi(1020)$, and J/ψ
H	Neutral mesons π^0, K^0, D^0, B^0, J/ψ, and $Y(1S)$
I	Neutral mesons π^0, K^0, D^0, B_s^0, J/ψ, and $Y(1S)$

	Quark Masses					
	m_1 (GeV)	m_2	m_3	m_4	m_5	d_{m0} (GeV^2)
A ([1] PDG)	0.00216	0.047	0.0935	1.273	4.813	
B ([3] Table 5.2)	0.6592	0.66135	0.7431	1.6215	4.7786	0.64113
C [~B]	0.65806	0.66047	0.742149	1.62171	4.77967	0.639932
D [$\phi(1020)$]	**0.612772**	**0.617715**	**0.70271**	**1.61737**	**4.80182**	**0.583976**
E [J/ψ]	**0.597813**	**0.604618**	**0.68971**	**1.61698**	**4.80862**	**0.566917**
F [$Y(1S)$]	0.695652	0.69160	0.776013	1.62459	4.76563	0.686478
G [ϕ, J/ψ]	0.607698	0.61752	0.70271	1.62224	4.80182	0.583976
H [J/ψ, $Y(1S)$, B^0]	0.642058	0.68017	0.726648	1.6403	4.76106	0.6428806
I [J/ψ, $Y(1S)$, B_s^0]	0.731953	0.816067	0.806536	1.68938	4.77819	0.806306

The new Cases H and I favor the heavy quarks c and b. But they led to pion masses 0.128 and 0.105, respectively, which are much smaller than those of the other cases and data. They are dropped.

Deviations of predicted meson masses from data [1] in [4] are somewhat smaller for Cases C, D and E. The quark masses above also show that they lie relatively close to each other, particularly for Cases D and E. Although Case C was designated as the "nominal" case in [4], Cases D and E will be adopted as the "mean

values" for the quark masses. This is justified by the requirement of using neutral mesons only as inputs mentioned above (2a).

The 5 neutral mesons used in Cases D-G contain 2 *u*'s, 3 *d*'s, 2 *s*'s, 1 *c*, and 2 *b*'s and constitute a balanced composition of the 5 quarks. Cases D and E contain $\phi(1020)$ with 2 *s* quarks and J/ψ with 2 *c* quarks, respectively. These masses lie around the middle of those of the 5 quarks. Cases D and E are written in bold face and will be used to predict meson masses for confrontation with data [1].

2.4. Predicted Meson Masses and Evaluation

Here, Sec. 5 "Special Case for Pions" in [4] will be employed. It shows that the classical relation $E_{10} = Q^2/R_m = 2.467$ MeV in (2b) is not valid for pions and is to be replaced by the SSI approximation given below (10) in [4]

$$E_1 = 4.6 \text{ MeV}. \tag{3}$$

By splitting up ρ and B^* in [4] to charged and neutral ones, there are now 18 mesons whose predicted mass using (2) and (3) are available for comparison with data. The results are shown in **Tables 2-5** below.

Table 2. (2) and (3) predictions for charged 0^- meson masses in GeV for Cases D and E in **Table 1**. E_0 is the measured meson mass [1]. E_{10} is the classical Coulomb energy in (2b); m_L is the mass of the lighter quark, m_{L0} is the mass of the same quark in **Table 2** in bold face; $\Delta_L = (m_L - m_{L0})/m_{L0}$ is the deviation from m_{L0} needed to match Data [1]. This is the worst case. Δ_H is the same as Δ_L but for the heavier quark; $L \rightarrow H$; Er = error of prediction; (2b) and (3) results have combined. Values in braces {…} not used; Δ_L% values from (2a) are given for reference but not used.

	$\pi^\pm$	$K^\pm$	$D^\pm$	$D_s^\pm$	$B^\pm$	$B_c^\pm$	
E_0 [1]	0.1395704	0.493677	1.86966	1.96835	5.27941	6.27447	
$E_0 - E_{10}$ (2b)	0.1371034	0.490773	1.86676	1.96645	5.27651	6.27157	
$E_0 - E_{10}$ (3)	0.134876						
Quarks	*u*, *d*	*u*, *s*	*d*, *c*	*s*, *c*	*u*, *b*	*c*, *b*	
Case D:							RMS%
E (2a)	0.134886	0.484345	1.87075	1.9715	5.27465	6.3016	
Er% E_0 [1]	−3.36	−1.89	+0.06	+0.16	−0.09	+0.43	1.6
Er% (2b)	{−1.62}	−1.31	+0.21	+0.26	−0.35	+0.48	
Er% (3)	+0.007						0.6
							Max $\lvert\Delta_L\rvert$%
E(2a)	m_L = 0.613295	0.616237	0.616805	0.6959	0.617413	1.5907	
Δ_L%	+0.085(*u*)	+0.57(*u*)	−0.15(*d*)	−0.97(*s*)	+0.76(*u*)	−1.65(*c*)	1.65(*c*)
(2b)	m_L = 0.613017	0.615153	0.614378	0.69841	0.69841	1.5879	
Δ_L%	{+0.04(*u*)}	+0.39(*u*)	−0.54(*d*)	−0.61(*s*)	+0.3(*u*)	−1.82(*c*)	1.82(*c*)
Δ_H%	{+0.04(*d*)}	+0.34(*s*)	−0.21(*c*)	−0.27(*c*)	+0.04(*b*)	−0.61(*b*)	
(3)	m_L = 0.61277						
Δ_L%	0(*u*)						

Continued

Case E:							RMS|%
E (2a)	0.134805	0.479634	1.87291	1.9731	5.2727	6.31335	
Er% E_0 [1]	−3.4	−2.8	+1.7	+0.24	−0.13	+0.62	1.95
Er% (2b)	{−1.7}	−2.3	+0.33	+0.34	−0.07	+0.67	
Er% (3)	−0.05						0.02
							Max $\|\Delta_L\|$%
(2a)	m_L = 0.598357	0.60311	0.60187	0.68565	0.60415	1.5786	
Δ_L%	+0.09(u)	+0.89(u)	−0.45(d)	−0.59(s)	+0.76(u)	−2.4(c)	2.4(c)
(2b)	m_L = 0.598073	0.602	0.59943	0.68402	0.68402	1.57576	
Δ_L%	{+0.043(u)}	+0.7(u)	−0.86(d)	−0.82(s)	+1.1(u)	−2.55(c)	2.55(c)
Δ_H%	{+0.043(d)}	+0.61(s)	−0.32(c)	−0.35(c)	+0.14(b)	−0.86(b)	
(3)	m_L = 0.597821						
Δ_L%	+0.001(u)						0.001

Table 3. (2) predictions for neutral vector 1^- mesons in GeV. The two ρ's refer to different production reactions. *denotes that the actual deviation is equally shared between both quarks due to symmetry. Other symbols have been defined in **Table 3**.

	ρ^0	ρ^0	K^{*0}	$\phi(1020)$	J/ψ	D^{*0}	B^{*0}	B_s^{*0}	$\Upsilon(1S)$	
E_0 [1]	0.77526	0.7692	0.89555	1.019461	3.0969	2.00685	5.32475	5.4154	9.4604	
Quarks	u, d	u, d	u, s	s, s	c, c	u, c	d, b	s, b	b, b	
Case D										RMS|%
E (2a)	0.76039	0.76039	0.8914	1.019461	3.0867	2.0094	5.33249	5.36693	9.5548	
Er% E_0 [1]	−1.92	−1.16	−0.46	0 input	−0.33	+0.13	+0.15	+1.0	+1.0	0.96
										Max $\|\Delta_L\|$%
(2a)	m_L = 0.62202	0.61824	0.61559	0.70271	1.6271	0.61049	0.6101	0.74998	4.70 (79)	
Δ_L%	+1.5(u)	+0.89(u)	+0.46(u)	0	+0.6(c)	−0.37(u)	−1.23(d)	+6.73(s)	−1.96(b)	
					(+0.3)*				(−0.98)*	1.5(u)
								+0.98(b)		
Case E										RMS|%
E (2a)	0.76038	0.76038	0.88885	1.0174	3.0969	2.0094	5.3325	5.36693	9.572	
Er% E_0 [1]	−1.92	−1.15	−0.75	−0.2	0 input	+0.13	+0.15	−0.9	+1.18	0.99
										Max $\|\Delta_L\|$%
(2a)	m_L = 0.60728	0.60341	0.60245	0.69122	1.617	0.59551	0.59699	0.73703	4.6975	
Δ_L%	+1.58(u)	+0.94(u)	+0.78(u)	+0.22(s)	0	−0.4(u)	−1.26(d)	+6.861(s)	−2.31(b)	6.86(s)
					(+0.11)*				(−1.16)*(b)	
1.58(u)										

The RMS% of the deviations of the predicted meson masses (2) from data [1] range from 0.9 to 1.95% and are improved relative to those in [4]. Using the (2b)

+ (3) values in Table 2 and values in Table 3, Table 4, the ranges of the deviations from the bold face "mean" quark masses in Table 1 needed to match the measured meson masses [1] are given in Table 5.

Table 4. (2) predictions for charged vector 1^- mesons in GeV. The two ρ's and two K^*'s refer to different production reactions. Other symbols have been defined in Table 3.

	$\rho^{\pm}$	$\rho^{\pm}$	$K^{*\pm}$	$K^{*\pm}$	$D^{*\pm}$	$D_s^{*\pm}$	$B^{*\pm}$	
E_0 [1]	0.77511	0.7665	0.89167	0.8955	2.01026	2.1122	5.32475	
Quark	u, d	u, d	u, s	u, s	d, c	s, c	u, b	
Case D								RMS|%
E (2a)	0.76039	0.76039	0.8914	0.8914	2.01487	2.10876	5.3275	
Er% E_0 [1]	−1.9	−0.8	−0.3	−0.46	+0.23	−0.16	+0.05	0.9
								Max $\|\Delta_L\|$%
(2a)	m_L = 0.62192	0.61656	0.61296	0.6156	0.61356	0.70584	0.6101	
Δ_L%	+1.5(u)	+0.62(u)	+0.3(u)	+0.45(u)	−0.67(d)	+0.4(s)	−0.44(u)	1.5(u)
Case E								RMS|%
E (2a)	0.760377	0.760377	0.88885	0.88885	2.017	2.1103	5.3256	
Er% E_0 [1]	−1.9	−0.8	−0.32	−0.74	0.33	0.2	0.016	0.9
								Max $\|\Delta_L\|$%
(2a)	m_L = 0.60718	0.6017	0.59976	0.60242	0.5986	0.6915	0.597	
Δ_L%	+1.57(u)	+0.65(u)	+0.33(u)	+0.77(u)	−1(d)	+0.26(s)	−0.14(u)	1.57(u)

Table 5. Error ranges for the deviations Δ_L% from the bold faced "mean" quark masses in Table 1 needed to match the meson data [1].

	Case D			Case E		
	Min	Max	Max − Min	Min	Max	Max − Min
(u)	−0.44	+1.5	1.87	−0.4	+1.58	1.98
(d)	−1.23	−0.54	0.72	−1.26	−0.86	0.4
(s)	−0.61	+6.73* (0)	7.34*	−0.82	+6.86* (0)	7.68*
(c)	−1.82	+0.6	2.4	−2.55	−2.55	0
(b)	−0.98	(+0.98)	0 (1.96)	−1.16	(+0.98)	0 (2.16)

The rather large 6.73* and 6.86*% are Δ_L% values for the c quark in B_s^{*0}. If Δ_H% for the b quark were adopted there, these * values reduce to 0, (0) above. At the same time, the accompanying b quark mass is increased by +0.98%, indicated by (+0.98) above.

The 2-digit accuracy of the quark masses in these tables improves the ±10% mentioned in [4], but remains far inferior than the 6-digit accuracies of the meson masses [1] that give rise to them. It refines the observation of the "variable" quark masses found in [4]. These masses vary within a few % from their "mean" masses in bold face in Table 1, dependent upon the flavor and spin of its companion

antiquark.

The bold faced "mean quark masses" themselves in Cases D and E in **Table 1** differ from each other also by −0.14 to +2.5% and by 3% for d_{m0} arising from the different mases of $\phi(1020)$ and J/ψ in **Table 1**. Case D is slightly better.

The new mean quark masses in Case D should replace those of Case B in **Table 1** which have been used to obtain the nucleon wave functions in Figure 11.1b [3]. This figure in its turn was used in (12.6.22) [3] to produce the average diquark-quark distance of 3.05 fm, widely used in cosmos (see the nucleon rod model in Sec. 5 below) and laboratory applications. This distance will be modified somewhat.

Quark masses are not natural constants, like the electron mass having a 9-digit accuracy. Contrary to an electron, a quark cannot exist alone and its mass hence cannot be measured. Nature is economical in providing natural constants. To give out many precise quark masses which cannot be measured and confirmed is uneconomical. Nature has found ways to comply to this principle via indefinite, *variable quark masses* and d_{m0} values utilizing the invisibility of quarks.

No analytic mass formula like (1) exists in the baryon sector. Only nucleon wave functions have been obtained employing the quark masses for Case B in **Table 1** and computer ([3] Ch 11).

This section supports SSI from laboratory data. Another support comes from the identification of nuclear force as Coulomb attraction between the u and d quarks in neighboring nucleons [6].

SSI is further supported in cosmos. The ratio of dark to ordinary matter is predicted to lie between 0 and ≈9 ([3] (15.3.4)), in near agreement with the observed ratio of 5. Another recent support is given in the following.

3. Black Neutron Star

3.1. Dark Matter and Rod Model of Nucleon ([6] Section 2.3)

In SSI, the equation of motion for the left-handed spinor ψ for quark B in a nucleon at x_{II} reads ([3] (15.1.1))

$$\partial_{II\dot{e}f}\psi_B^f\left(x_{II}\right)-i\left(V_{BC}\left(x_{II}\right)+V_{BA}\left(x_{II}\right)+V_{BG}\left(x_{II}\right)\right)\chi_{B\dot{e}}\left(x_{II}\right)=im_B\chi_{B\dot{e}}\left(x_{II}\right) \quad (4a)$$

$$V_{BG}\left(x_{II}\right)=-\frac{GM_g m_B}{\left|\underline{x}_{II}\right|} \quad (4b)$$

where the m's are the quark masses, G the gravitational constant, the first two V's are the scalar strong interquark potential between quark B and the other two quarks A and C at x_I and x_{III}, respectively. V_{BG} is an ambient, perturbative gravitational potential emanating from a large mass M far away at $\underline{x}_{II}=0$. There is also a similar equation for the right-handed spinor χ. The dotted and undotted spinor indices $e, f\ldots$run from 1 to 2.

Two similar sets of equations like (4) also hold for quarks A and C with $x_{II}\to x_I$ and x_{III}, respectively. The differences between these 3 $\underline{x}$ values are small, of the order of fm, but these $\underline{x}$ values themselves are large, of the order of light years. Therefore, $|\underline{x}_{II}|$ in (4b) can be replaced by their mean value $|\underline{X}|$ in the laboratory

frame.

Gravity is naturally included and acts on all quarks in (4) and their sister equations directly as well as on X and on the relative, hidden coordinates $x = x_{II} - x_I, \ldots$ From the equations mentioned above, wave functions of nucleons have been constructed. At rest, these contain a time dependences of the form $\exp(-iE_0X^0 + i\omega_0x^0)$. E_0 is the nucleon mass, X^0 the laboratory time and ω_0 the relative energy and x^0 the relative time between the quarks, respectively. Gravity affects them all. $-\omega_0 < 0$ has been identified as dark matter and the positive relative energy PRE $-\omega_0 > 0$ as dark energy ([3] (15.3.3)).

The radial part of these wave functions depends upon the distance $|\underline{x}| = r$, the diquark-quark separation. The average of this separation obtained from these functions is 3.05 fm. Instead of the cumbersome wave functions, the neutron is modeled heuristically as a rigid rod of length 3.05 fm with a dd diquark and a u quark at its ends ([6] Section 2.3), as is illustrated by the arrow in **Figure 1**.

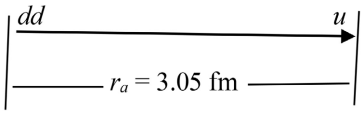

Figure 1. Rod model of neutron. Arrow shows spin orientation.

For the proton, $d \leftrightarrow u$. Including the wave functions, the nucleon has an elliptical form with both quarks near the focal points in the hidden, relative space $\underline{x}$.

3.2. Black Neutron Star and S250206dm Kilonova

A neutron star at the Tolman, Oppenheimer, Volkoff or TOV limit starts to collapse into a black hole according to general relativity in which matter is a continuum. But this theory breaks down at very small distances where the discrete neutron rods prevail. When a new neutron rod arrives at the surface of such a neutron star, it becomes too heavy and starts to fall towards its center, In SSI ([5] Sec. 7), ([3] pp. 270-271), however, this fall is accompanied by generation of dark matter which exactly cancels the gravitational energy gain during this fall, The fall stops and the new neutron remains in limbo on its surface. Additional new neutrons arriving behave similarly and the star becomes a "black neutron star" BLNS (not to be confused with BNS = binary neutron star in the literature) which has a mass of ≈ 3.65 solar mass M_{SUN} and a radius of 10.8 km ([3] pp. 270-271), ([5] Sec. 7).

In the recent event [7] ([2] List of Gravitational Wave Observations S250206dm), a "trifecta" kilonova was observed by LIGO (gravitational wave), ICE Cube (neutrino) and CHIME (Fast Radio Burst).

According to the AI site Big Think, S250206dm is an event that definitely contains a neutron star and that either represents a neutron star-neutron star or neutron star-black hole merger, with a combined mass that's on the relatively low end: no more than five solar masses and possibly as low (or lower than) three solar masses (corrected to between 3.5 - 5 solar masses).

The expected black hole according to general relativity was not found but a mass gap was seen. The observed results favor the existence of a BLNS with mass 3.5 - 5 M_{SUN}. This interpretation is compatible with the predicted 3.65 solar masses above in 2019 [5] and supports SSI.

An additional support ([2] List of Gravitational Wave Observations GW230529) shows that the primary object in lower mass-gap is 3.6 M_{SUN}.

3.3. Model of Heavier Black Neutron Stars

3.3.1. Idealized Model

The mass of the above BLNS is limited to about 3.6 M_{SUN}. To investigate whether BLNS can exist for heavier neutron stars, the following idealized scenario will be considered. A perfectly spherical neutron star NS_{TOV} having a mass M_{TOV} and radius R_{TOV} is on the verge of its TOV limit. An external neutron, represented by the rod model of **Figure 1**, arrives at this star NS_{TOV} with its *dd* diquark landing on its top surface, as is shown in **Figure 2**. The rod's spin arrow points upwards ([3] Fig. 15.3), ([5] Fig. 2). Many other external neutrons also landed similarly, as are illustrated by 7 of them in **Figure 2**.

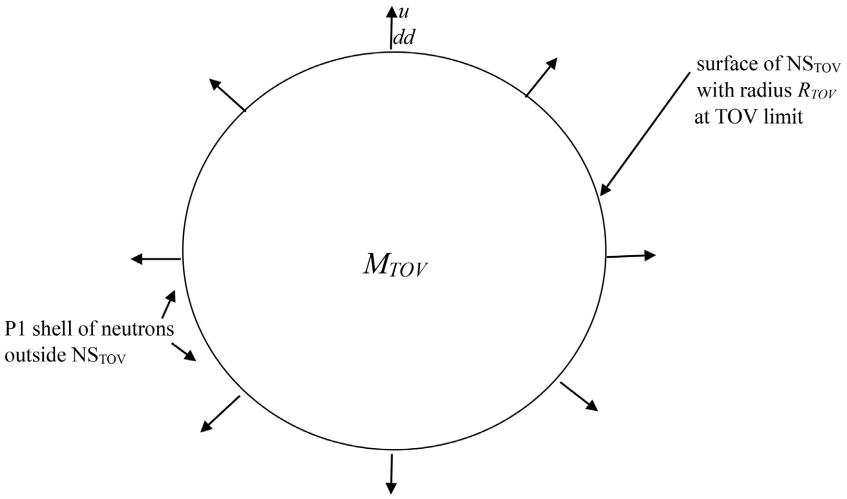

Figure 2. Schematic view of a neutron star NS_{TOV} at its TOV limit with mass M_{TOV} and radius R_{TOV}. An external neutron, illustrated by a short arrow here to represent the neutron rod in **Figure 1**, arrives and is attracted to this NS_{TOV} with its *dd* diquark landing on the top surface of this NS_{TOV} and its spin vector pointing outwards. Other new neutrons arrive and are attached to other parts of this spherical surface, illustrated by 7 other arrows. When this surface is fully populated by new incoming neutrons, a neutron shell, indicated by P1 shell, is formed outside this NS_{TOV}.

To achieve heavier neutron stars, more neutrons are needed. Their sources are interstellar gas and debris and smaller stars and their planets near this NS_{TOV}. Since nuclei are formed via Coulomb attraction between *u* and *d* quarks in neighboring nucleons [6], such bounds can be broken at high temperatures and in the strong gravitational field near this NS_{TOV}.

As more new neutrons arrive, they will fill up the remainder of the free surface

area of this NS_{TOV} to form a P1 shell indicated in Figure 2. This NS_{TOV} with this P1 shell now becomes too heavy and tends to collapse towards its center. But this collapse does not happen according to Sec. 6 and this NS_{TOV} + P1 shell become a BLNS. Additional incoming neutrons form new shells, P2, P3…Pν on this P1 shell.

3.3.2. Densities of the P1, P2, … Pν Shells

The density $\rho_{TOV} \approx 1.36 \times 10^9$ kg/m^3 of NS_{TOV} has been estimated from $M_{TOV} = 3.6\ M_{SUN}$ and $R_{TOV} = 10.8$ km of the BLNS in Sec. 6. It corresponds to that a neutron occupies (1072 fm)^3. The densities of the P1, P2, … Pν shells are unknown and are related to the problem that the equations of state of extremely dense matter are not well known, mentioned near the end of p 270 in [3]. It has to be estimated indirectly.

As all the neighboring neutrons in the P1 shell have the same spin orientation polarized by the gravitational field of this NS_{TOV}, they repel each other electrostatically and by Pauli's principle. This in contrast to the neutrons inside this NS_{TOV} where two neighboring neutrons may have opposite spin directions (see Figure 1) and hence attract each other electrostatically and can be closer to each other.

Therefore, the density ρ_P of the P1, P2, … Pν shells may be expected to be lower than ρ_{TOV}. Including these ν shells, the radius of such a neutron star $BLNS_\nu$ is $R_{BLNS,\nu} = R_{TOV}$ + thickness of the ν shells. To arrive at an estimate, assume the phenomenological density distribution

$$\rho_P(R) = \left(1 - \left(R/R_{BLNS,\nu}\right)^\alpha\right)\rho_{TOV},$$
$$R = \text{radius from the center of BLNS}_\nu,\ \alpha = \text{constant} \tag{5}$$

For $\alpha \ll 1$, ρ_P drops very sharply from ρ_{TOV} at $R = R_{TOV}$ as R increases. The drop is linear for $\alpha = 1$ and approaches a step function with $\rho_P \approx \rho_{TOV}$ for $\alpha \gg 1$.

3.3.3. Radius and Schwarzschild Radius

Including at first only the P1 shell, the NS_{TOV} becomes a heavier black neutron star $BLNS_{P1}$. Its Schwarzschild radius $R_{SchBLNS,P1}$ is proportional to the mass of this star. Let the P1 shell mass be $\Delta_{P1} M_{TOV}$ and the radius of $BLNS_{P1}$ be R_{TOV+P1}, one finds

$$R_{SchBLNS,P1} = (1 + \Delta_{P1}) R_{TOV} \tag{6a}$$

$$R_{TOV+P1} = \left(1 + \frac{\rho_{TOV}}{\rho_{P1}}\Delta_{P1}\right)^{1/3} R_{TOV} \tag{6b}$$

which holds generally for arbitrary Δ_{P1} values.

As more shells P2, P3…Pν are superimposed upon the P1 shell in Figure 2, they become very thick and dominate over R_{TOV+P1} for large ν values to form a new, more massive neutron star $BLNS_\nu$, with $R_{TOV+P1} \to R_{BLNS,\nu}$, $R_{SchBLNS,P1} \to R_{SchBLNS,\nu}$, $(1 + \Delta_{P1}) M_{TOV} \to M_{BLNS,\nu}$, and $\rho_{P1} \to \rho_P(R)$ in (5). The mass of this heavier $BLNS_\nu$ is

$$\begin{aligned} M_{BLNS,\nu} &= M_{TOV} + \int_{R_{TOV}}^{R_{BLNS,\nu}} \mathrm{d}R 4\pi R^2 \rho_P(R) \\ &= 4\pi\rho_{TOV}\left[\frac{x^3 - 1}{3} - \frac{x^3 - x^{-\alpha}}{\alpha + 3}\right] R_{TOV}^3,\ \ x = \frac{R_{BLNS,\nu}}{R_{TOV}} \end{aligned} \tag{7}$$

which fixes the radius $R_{BLNS,\nu}$ and the Schwarzschild radius $R_{SchBLNS,\nu}$ of this BLNS$_\nu$. The results are shown in Table 6.

Table 6. Radii $R_{BLNS,\nu}$ and Schwarzschild radii $R_{SchBLNS,\nu}$ of massive black neutron stars BLNS$_\nu$ as function of their masses $M_{BLNS,\nu}$ from (7). The braced entry {23} shows that it exceeds its $R_{SchBLNS,\nu} = 21.6$ and hence is not "black".

	Input	BLNS	BLNS	BLNS	MBLNS	Supermassive BLNS
$M_{BLNS,\nu}$ (unit M_{SUN})	3.6	7.2	18	3.6×10^2	3.6×10^3	3.6×10^9
$R_{SchBLNS,\nu}$ (km)	10.8	21.6	54	1080	10,800	10.8×10^9
$R_{BLNS,\nu}$ (km)						
$\alpha = 100$ ($\rho_P \approx \rho_{TOV}$)	10.8	14	13	51	109	10,897
$\alpha = 1$ (linear decrease)	10.8	20	29	79	172	17,140
$\alpha = 1/2$ (sharp decrease)	10.8	{23}	34	96	206	20,660

This table shows that the Schwarzschild radii $R_{SchBLNS,\nu}$ far exceed the radii of the corresponding BLNS$_\nu$, especially for the supermassive BLNS. One exception is that given in braces {}, which is not "black", for a NS with only twice the mass of the NS$_{TOV}$ in Sec. 6 for sharply decreasing density ρ_P with $\alpha = 1/2$. Such a small departure from the TOV limit of M_{TOV} is however removed when this neutron star with mass $2M_{TOV}$ a) is allowed to grow a little to, say, $2.5M_{TOV}$ or b) its density decrease is less sharp with $\alpha \approx$, say, 0.6 instead.

The density distributions in such BLNS$_\nu$ are unknown and cannot be known. But the Schwarzschild radii exceed the BLNS$_\nu$ radii in Table 6 by so large margins that whatever these distributions are, these BLNS$_\nu$, especially the supermassive ones, will remain black.

3.3.4. "Peach" Model of BLNS and Supermassive BLNS

The spherical shell P1 in Figure 2 and the additional shells P2, … Pν do not affect the interior of the core NS$_{TOV}$ which remains as it was when it was formed. Thus, all conventional black holes are actually BLNSs, including supermassive ones, having a core of NS$_{TOV}$, a BLNS at its TOV limit in Sec. 6 and Figure 2, at their centers. *The gravitational singularity in a black hole from general relativity is replaced by such a dense NS$_{TOV}$ core with a radius* ~11 *km*. This configuration may be nicknamed a "peach" (or avocado) model, with the peach's hard kernel representing the dense NS$_{TOV}$ core. Removal of gravitational singularities in this model renders it to be compatible with quantum mechanics.

3.4. On Quantum Gravity

Such a compatibility is a basic ingredient in an eventual quantum gravity theory. SSI appears to provide a natural basis for such a theory. It is a quantum mechan-

ical theory and its scalar strong interaction is compatible with that of Newtonian gravitation, as is seen in (4).

One approach may be to start from quark equations of motion of the form (4), where the scalar gravitational potential $V_{BG}(x_{II})$ may be generalized to gravitational tensors. This calls for that the other terms in (4) also need be generalized to tensors. For compatibility with SSI, such tensors need be converted to spinor form, similar to the conversion of the Maxwell equations in tensor form to van der Waerden's spinor form [8]. Quark coordinates of types x_I, x_{II}, … need be decomposed to a laboratory coordinate X and relative, hidden coordinates between quarks in which strong interquark interactions take place. Such a scenario appears to be extremely complicated.

4. SSI Conception of the Universe

Support of SSI in the above two sections leads to the need for a modified conception of the universe.

4.1. SM vs SSI

Currently, we have 4 basic forces, strong, electromagnetic, weak, and gravitational. In the standard model SM [2], the strong force between colored quarks is mediated by vectorial gluons. The nuclear force is attributed to some unspecified remnants of such strong forces. The electromagnetic and weak interactions merge into a common electro-weak interaction at $\rho_H = 246$ GeV of the Higgs wave function. Although the Higgs boson was originally introduced to provide mass to the massless gauge bosons $W^{\pm}$ and Z. So, the 4 fundamental forces are reduced to 3. At low energy, however, the weak charge g and the electric charge e, related by the Weinberg angle, are too close to each other to give rise to basically different couplings. All interactions take place in the laboratory space X.

The above 4 basic forces are also present in SSI, but with different content. The strong force is scalar and holds the quarks together in their "hidden" (with respect to electromagnetic interactions), relative space x absent in SM. The nuclear force is of Coulomb origin [6] acting between the fractional charges of the u and d quarks in neighboring nucleons in visible laboratory space X. The strong coupling in laboratory space is given by ([3] (8.3.11))

$$\alpha_s = \alpha^{-1/4} = g_s^2/4\pi = 0.2923 \tag{8}$$

where g_s is the strong coupling between 2 quarks ([3] (2.1.2)) which is related to the electromagnetic coupling or fine structure constant $\alpha = e^2/4\pi = 1/137$. As this value is of the same magnitude as (8), both may be considered as one single electro-strong coupling constant.

The corresponding weak coupling is ([3] (7.5.22a))

$$F_W^2 = 8.0314\times10^{-14} \propto G^2 \tag{9}$$

where G is the Fermi constant ([3] (7.5.21)). The gravitational coupling is of the order 10^{-39}. Thus, there are also 3 basic coupling constants but their orders of

magnitudes are now clearly separated:

$$\sim 10^{-1} : 10^{-13} : 10^{-39} \quad \text{for} \quad \text{electro-strong} : \text{weak} : \text{gravitational} \qquad (10)$$

coupling strengths, in contrast to the electro-weak coupling in SM. In SSI, the Weinberg angle is predicted. The gauge boson mass M_W is inherently generated by $\int \mathrm{d}x^0 \Big/ \int \mathrm{d}\underline{X}^3 \to \infty/\infty \propto M_W^2$ ([3] (7.4.6b)), where x^0 is the relative time between the quarks.

4.2. Interrelations between the Building Blocks and Their Interactions

Figure 3 shows the basic constituents in the universe and the interactions between them.

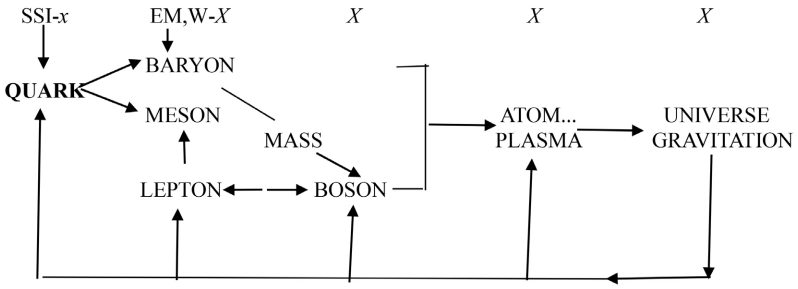

Figure 3. Outline of basic constituents in the universe and their mutual relations. QUARK: *u*, *d*, *s*, *c*, and *b* quarks and their antiparticles; BARYON: limited to nucleons here, diquark and quark confined by scalar strong interaction; MESON: quark-antiquark confined by scalar strong interaction; BOSON: Photon, $W^{\pm}$ and Z; LEPTON: $e^{\pm}$, $\mu^{\pm}$, $\tau^{\pm}$, and their associated neutrinos; SSI-x: Scalar Strong Interaction between two quarks in their relative space x invisible from the laboratory space X in which EM,W-X take place; EM, W-X: Electro-Magnetic and Weak interactions in laboratory space X; MASS: relative time between quarks provides MASS to $W^{\pm}$ and Z.

Differences of SSI and Standard Model SM are:

1) SSI-x: quarks interacting strongly in "hidden", relative space x. This is replaced by vectorial gluons interacting with colored quarks in laboratory space X in SM;

2) MASS arrow is replaced by an extra particle, the Higgs boson, in SM;

3) GRAVITATION acts on quarks directly, not so in SM;

4) Nuclear force originates in Coulomb interactions between quarks in neighboring nucleons. In SM, such force is assigned to remnants of the color-forces in 1. above but unspecified.

The absence of a gravitational singularity in our universe in Section 3.3.4 casts a doubt on the "big bang" hypothesis of the birth of our universe. But no alternative is offered.

Consider a hydrogen atom in the outer edges of the universe. It experiences a collision with another hydrogen atom that causes its electron sphere to move towards the center of the universe. The proton in it follows suit.by virtue of their Coulomb bond in the laboratory space X. The heavier quarks lag behind. In this

situation, the relative energy between the quarks turns positive and this causes the gravitational force on them to switch sign; an antigravity move outwards from the center of the universe ensues and will continually do so until another collision takes place.

Some scenarios of the antigravity expansion of the universe are given in ([3] Sec. 16.4). In one of them, the universe's outer part will expand forever but get thinner all the time. Its inner part may however be intact. But as hydrogen gas is used up, the universe may become dark and lifeless. Like many other scenarios, this one is speculation. No calculations have been carried out regarding this case.

Another one calculated with computer is given by ([3] Table 16.1) where the Hubble parameter increases from the present Hubble constant H_0 to a maximum of $\sim 2 \times !0^3 H_0$ after 10^7 years and then will return to $\sim 1.5 H_0$ after $!0^{10}$ years.

Acknowledgements

Section 2 was initiated by Albin Hoh, a Bitcoin expert grandson, who informed me about the kilonova S250206dm and provided me with material on its interpretation. His father, Eric Hoh, meant that a single possible existence of a black neutron star created a billion years ago is not a strong enough verification of the 2019 prediction and asked whether heavier black neutron stars may exist. This led to the "peach" model for all black neutron stars and black holes in general in Section 3.3.4.

This paper is dedicated to my late wife Birgitta, who passed away last month. Without her support, SSI would not have been created.

Conflicts of Interest

The author declares no conflicts of interest regarding the publication of this paper.

References

[1] Particle Data Group (2025). https://pdglive.lbl.gov/

[2] Wikipedia (2025). https://en.wikipedia.org/wiki/Main_Page

[3] Hoh, F.C. (2022) Scalar Strong Interaction Hadron Theory III. Nova Science Publishers. https://doi.org/10.52305/xuvv2113

[4] Hoh, C.F. (2019) On Variable Quark Masses Derived from Meson Spectra. *SCIREA Journal of Physics*, **9**, 245-255. https://doi.org/10.54647/physics140661

[5] Hoh, F.C. (2019) Cosmic Applications of Relative Energy between Quarks in Nucleons. *Journal of Modern Physics*, **10**, 1645-1658. https://doi.org/10.4236/jmp.2019.1014108

[6] Hoh, F.C. (2024) On U-D Quark Coulomb Origin of Nuclear Force. *Physical Science International Journal*, **28**, Article ID: 111106. https://doi.org/10.9734/psij/2024/v28i1816

[7] Hoh, A. (2025) Private Communication from AI.

[8] Laporte, O. and Uhlenbeck, G.E. (1931) Application of Spinor Analysis to the Maxwell and Dirac Equations. *Physical Review*, **37**, 1380-1397. https://doi.org/10.1103/physrev.37.1380